Production and Confinement of Electron Cyclotron Resonance Plasmas in the WIIa-Stellarator

R.A. Ellis, Jr.[x] and D. Eckhartt

IPP 2/85

July 1970

INSTITUT FÜR PLASMAPHYSIK

GARCHING BEI MUNCHEN

INSTITUT FÜR PLASMAPHYSIK
GARCHING BEI MÜNCHEN

Production and Confinement of Electron Cyclotron Resonance Plasmas in the WIIa-Stellarator

R.A. Ellis, Jr.[x] and D. Eckhartt

IPP 2/85 July 1970

[x] Permanent address: Plasma Physics Laboratory
Princeton University
Princeton, N.J., U.S.A.

Die nachstehende Arbeit wurde im Rahmen des Vertrages zwischen dem Institut für Plasmaphysik GmbH und der Europäischen Atomgemeinschaft über die Zusammenarbeit auf dem Gebiete der Plasmaphysik durchgeführt.

IPP 2/85 R.A. Ellis, Jr.
D. Eckhartt

Production and Confinement of Electron Cyclotron Resonance Plasmas in the WIIa-Stellarator.

July 1970
(in English)

Abstract

Preliminary measurements of noble gas plasmas generated by low power c.w. ECR have been made in the stellarator WIIa. Densities were in the range 10^8 to 10^{10} cm^{-3} and electron temperatures ranged from 4 to 11 eV. The general features of the density versus transform curves are quite similar to those observed with Barium plasmas produced by contact ionization. The confinement time is estimated to be about 10 Bohm times. The discharges, in general, are turbulent and show fluctuations in the range expected for drift waves. A comparison is made with the results obtained in other stellarators.

1. Introduction

The confinement of low density alkali and alkaline earth plasmas produced by contact ionization in the WI and WII stellarators has been interpreted as approaching the classical collisional limit for fully ionized axisymmetric plasmas and, in any case, exceeds the Bohm value by one to two orders of magnitude.[1,2] The extension of these measurements to other regions in parameter space has obvious importance. This extension could take many directions, including wider ranges of density, temperature, and magnetic field.

This report is concerned with production and heating of plasmas with higher densities and temperatures by means of low power c.w. electron cyclotron resonance (ECRH). The electron temperatures are in the range 3 to 11 eV and the charged-particle densities cover the range 10^8 cm^{-3} to 10^{11} cm^{-3}. The percentage ionization ranges from 0,001 to 10 percent, depending on neutral pressure and power input. The ion temperature is presumably comparable with the gas temperature. The plasmas created by ECRH are interesting primarily because they have electron temperatures, electron densities, and neutral gas densities comparable with plasmas produced in other stellarators by external injection, thus permitting some comparison of performance among different stellarators.[3-8] A second significant attribute of plasmas produced by ECRH is that they simulate quite well the plasmas which can be produced by further heating of presently available alkali and alkaline-earth plasmas produced by contact ionization.

The production of plasmas by the action on neutral gas of a low power microwave field which pervades the entire volume of the stellarator inevitably yields a plasma during the powered phase in which electron-neutral collisions dominate the processes. However, it should be noted that this will probably be the case for the first experiments in further heating of plasmas produced by contact ionization or by photo-ionization because the pressure of the background gas is usually comparable with the minimum pressure at which it is possible to produce discharges by ECRH.

The experiments described herein are preliminary, but it is a simple matter to refine and extend them and to obtain a fairly complete picture of the con-

finement of such plasmas in the WII stellarator. We will discuss in turn the general experimental arrangement; the properties of the discharges; the power balance and estimates of confinement; fluctuations; and finally, relation of these results to those obtained on other stellarators with comparable dimensions, magnetic fields and plasma electron densities and temperatures.

2. Description of the apparatus and techniques

The experiments were carried out in the WIIa stellarator, which is shown schematically in Figure 1. This is a circular stellarator with a stainless steel vacuum tube of 12 cm minor diameter and 1 meter major diameter. An internal annular gridded particle detector limits the maximum aperture to 10 cm diameter. The rotational transform is provided by five periods of $\ell = 2$ helical windings uniformly covering the torus with an effective radius of ≈ 12 cm. The rotational transform t^*, which can be produced is a function of the main confining field because of power and cooling limitations associated with the helical windings and in the experiments performed here, had a maximum value of 0.65. The main confining field was operated continously for these experiments. The helical windings could be operated with a constant current or with a programmed variation of the current.

The base pressure was normally between 4 and 8×10^{-7} torr. All pressures were measured with a conventional Bayard-Alpert gauge.

The microwave power was provided by various magnetrons and klystrons. The minimum power required was only 20 to 40 milliwatts and the maximum power available was about 16 watts. The frequencies were measured with cavity wave meters. The absolute power was determined by standard techniques using calibrated bolometers and has the accuracy of the manufactures which is about 10%. The stated values of power are those measured near the power sources. The microwave circuit is shown in Figure 2.

---

t^* is defined as $\frac{\iota}{2\pi}$, where ι is the usually defined rotational transform.

There is at least 3 dB of attenuation in the 10 meters of wave guide connecting the microwave oscillators with the stellarator and an unknown loss in the vacuum window. The power is radiated from an open X-band wave guide which is directed such that E is nearly perpendicular to the toroidal magnetic field. The reflected power was also measured and found to be about ten percent with only small variations as a function of plasma density. The behavior of the reflected power suggests that the vacuum vessel behaves like a low Q resonator which is to be expected because there are several ports which are large enough to transmit freely the microwave radiation at the frequencies which were used.

All densities and temperatures were determined from cylindrical Langmuir probes with tips 0.1 mm in diameter and 4 mm long. The insulator was a 0.5 diameter ceramic tube. The length to radius ratio is 80 which permits the evaluation of density according to the theory of the infinite cylindrical probe.[9] The probes were located about 20^0 below the horizontal plane and could be moved radially on a diameter.

Measurements of the time decay of the plasma were made by switching off the high voltage of the 9.2 GHz magnetron and observing the decrease of the probe current. The time decay of the microwave power was measured to be less than 5 usec.

Measurements of the spectrum of density fluctuations, i.e., ion current fluctuations were obtained with the aid of Tektronix Type 115 Spectrum Analyzer.

3. General characteristics of the discharges

The discharges were produced in Argon and Xenon in the pressure range from 2×10^{-6} to 10^{-4} torr. A typical curve of the variation of electron density, n_e, near the center of the discharge tube as a function of t is shown in Figure 3 for an Argon discharge. Measurements of the electron temperature, T_e, near the axis at a few values of t indicate, that T_e is not a strong function of t for fixed microwave power and neutral pressure. Figure 3 shows a striking similarity to the n_e-t

curves obtained for a Barium plasma produced by contact ionization[10]; in particular, the behavior at rational values of ι is essentially the same for this plasma which is produced in a quite different manner and which has a much higher electron temperature. There is also the same disagreement with the numerical calculations of ι which was observed in the Barium plasmas.

An example of the variation of density and temperature with radius is shown in Figure 4. The form of this curve is quite typical except for very low ι and for data obtained at higher power when $\iota \approx 0.5$ which show broader and more asymmetrical profiles. From such radial density profiles data a plot of the full-width at half maximum is shown in Figure 5. The initial decrease is qualitatively explained by the increasingly elliptical shape of the magnetic surfaces as ι increases.

From data similar to that shown in Figures 3 and 4 we obtain the variation of electron temperature and density with power at fixed ι and Argon in Figures 6 and 7. These data should be considered "typical" in some sense because it is clear from Figure 3 that the density varies considerably with ι for fixed power and neutral pressure, although the electron temperature is almost constant.

It should be pointed out that at low power (< 1 watt) and pressure ($< 10^{-5}$ torr) there is no plasma produced in the stellarator at $\iota = 0$ and near some rational values of ι, particularly at $\iota = 1/2$ and $1/3$. However, at higher power levels and pressures, it is possible to produce a discharge at all values of ι. The observed range of magnetic field at which breakdown occurred at power levels smaller than 300 milliwatts corresponded to the condition that the magnetic field for electron cyclotron resonance should intersect the volume within one or two cm of the axis of the vacuum vessel.[11]

The discharges in Argon and Xenon are, in general, quite similar with regard to n_e and T_e for comparable power level and pressures. Typical discharge properties are summarized in Table 1.

The discharges in general, exhibit fluctuations which will be discussed in Section 6.

Rough measurements of the space potential in a few cases indicate that the plasma is charged positively which implies that the electrons have a higher intrinsic loss rate.

Figure 8 shows a plot of density vs. t for a discharge in Xenon which exhibits maxima near rational values of t. superimposed to the general feature of broad minima near $t = 1/3$ and $1/2$. Similar curves have been obtained for a certain range of parameters in Xenon. The appearence of these relative maxima is of particular interest in view to the various ideas proposed to explain the increased plasma losses for rational values of t.

4. Estimates of confinement times during steady state operation

In steady state operation, the average confinement time, τ , is determined by dividing the total number of particles present by the rate of production of particles. The number of particles present can be determined with relative ease, but in ECRH discharges the production rate is more difficult to determine. There are two approaches which enable one to estimate the production rate: first, from the absolute power, one can determine an upper limit to the flux by assigning a minimum energy of production to each electron and dividing the input power by this energy per electron-ion pair. A second method is to assume a Maxwellian electron velocity distribution and compute the production rate from the known ionization cross-sections and measured electron densitites and temperatures. This difficulty in determining the flux would seem to be a disadvantage when compared to the ease of determining the production rate in plasmas generated by photo ionization and contact ionization, but this is easily seen to be illusory when we remember that the ECRH plasmas have larger electron temperatures at which the situation is rather similar for all modes of plasma production.

For a few cases, we have carried out the estimates of confinement times outlined in the previous paragraph. As an example, let us consider an Argon discharge with neutral pressure 6×10^{-6} torr, maximum electron density 3.8×10^{8} cm^{-3}, total number of particles 1.25×10^{12}, and input

power 40 milliwatts. The radial variation of the important quantitites is shown in Figure 9. The upper limit to the particle production rate is 5.0×10^{15} sec^{-1} obtained by assuming 50 eV/ion pairs and the full 40 milliwatts. (We have not corrected for waveguide losses, reflections, or efficiency of coupling.) These assumptions lead to a minimum life time of about 250 μsec which can be compared with an estimated Bohm time of about 160 μsec. The Bohm time, τ_B, is given by $\tau_B = \frac{28\,Br^2}{T_e}$ μsec for a Bessel type density profile.
We have put $r^2 = 15$ cm^2 because of the rather steep density profile. The other relevant numbers are $B = 3.2$ k gauss and maximum $T_e = 8.6$ eV. It should be emphasized that the above life time is an under-estimate and that the known corrections would allow - perhaps several - factors two of increase, but probably not several orders of magnitude. Thus, we can resonably estimate on this basis that the confinement time in this case is about an order of magnitude greater than the Bohm time, but probably not two orders greater.

The second type of estimate has also been carried out for the same discharge with the aid of the rate coefficients, $\overline{\sigma v}$, computed by Lotz,[12] where the bar denotes an average of the ionization cross-section over a Maxwellian distribution at some specified temperature. This calculation involves evaluating the following integrals:

$$\tau = \frac{N}{\phi} = \frac{\int n_e dV}{n_o \int n_e \cdot \overline{\sigma v} \cdot dV}$$

where N, ϕ, n_e, n_o are, respectively, the total number of particles, the total production rate, the electron density, and the neutral gas density. For the discharge of Figure 9, we obtain $\phi = 1.25 \times 10^{15}$ sec^{-1} and again $N = 1.25 \times 10^{12}$ which gives $\tau = 1.0$ msec about four times larger than the value given in the preceeding paragraph. This estimate should be more reliable and can also be an under-estimate, but it is not likely to be more than a factor ten too low. The largest uncertainity lies in the assumption of a Maxwellian velocity distribution for the electrons. Here, the expectation is that the high energy tail would be somewhat depleted because of the

inelastic processes while, at least for the case considered above, there is an insufficient number of collisions to fill this part of the distribution. However, it is possible that the ECRH production process favors the production of fast electrons which would tend to compensate (even over-compensate) the effect of the inelastic processes.

The maximum number of fast electrons can be estimated by attributing all of the production rate to fast electrons. We consider the estimated production rate obtained from the incident power and compute the density of fast electron which would account for this production rate. The assumption is made that the ionization cross-section, σ_i, varies as $\frac{1}{v}$ for electron velocities larger than the velocity at maximum σ_i. Therefore, the rate coefficient is almost constant for electrons with energies higher than 100 eV and we define fast electrons to be those with energies greater than 100 eV. The computed density of "fast electrons" for the case considered above is about 6×10^6 cm^{-3} which is much less than the observed densities. From this we conclude that the velocity distribution cannot be grossly dominated by energetic electrons.

The confinement times, τ, which have been evaluated as indicated above are given in Table 1 together with the relevant plasma parameters. τ_B denotes the corresponding Bohm times.

5. Measurements of the density decay after termination of the ECR heating pulse

A second and perhaps more convincing measurement of the confinement time is the observation of the density decay after switching off the microwave power. Typical oscilloscope traces of such decays are shown in Figure 10. From a series of such measurements at different values of t we obtained Figure 11 which shows the curve of decay time, τ, versus t for Argon at a pressure of 2×10^{-5} torr and at a power of 100 milliwatts. Also shown in Figure 11 is a curve of the density on the axis just proir to the interruption of power.

These data suggest that the decay time is largest when the density is highest. It should be stressed that the τ's are the initial decay rates and do not include "tails" which have much longer decay times. A proper interpretation of these data, which are ion saturation current traces, requires a determination of T_e versus time during the afterglows because the ion saturation current is proportional to $n_e T_e^{1/2}$. Other experiments show that the cooling of afterglows is fast which implies that the decay times given here are different from the real density decay times. The likelihood is great that the afterglows with decay times shorter than 1 msec are almost isothermal while those longer than 2 or 3 msec exhibit some effects of cooling.

The magnitudes of the decay times, particularly for the cases when the density is relatively high are somewhat larger but lie well within the limits estimated for the steady state discharges given in Section 4. Thus, we have again a result which gives confinement times of about 10 Bohm times.

Similiar results have been obtained in both Argon and Xenon discharges, including a study of the variation with neutral pressure between 5×10^{-6} and 10^{-4} torr. The results for Argon at several pressures are shown in Figure 12. There is a tendency for a maximum in τ to occur at $t \approx 0.3$. The relation of these data to the question of trapped particles will be discussed in Section 8.

6. Fluctuations

The $\ell = 2$ helical windings on WIIa produce very low shear; the transform increases from the axis to the aperture by only 5 per cent when t is 0.5 and is less for smaller t. Thus, the reported absence of fluctuations in the contact ionization plasmas is something of a surprise because for these plasma parameters, drift waves should be unstable.[13]

The situation with the ECR plasmas is quite different. The general case is that fluctuations are present with $\frac{\delta n}{n}$ at the axis typically 10-20%. The general character of the fluctuations can already be seen in Figure 10

which shows the last part of the ECR-discharge before the power is switched off. In Figures 13 and 14 we show spectra of the fluctuations present in Argon and Xenon discharges. The difference between Argon and Xenon is the tendency for the Argon Fluctuations to be turbulent while the Xenon fluctuations are almost monochromatic. An exception in Argon occurs near the $\iota = 0.5$ degeneracy where the Argon fluctuations are almost monochromatic for this particular combination of confining field, power, pressure, and ι.

The tendency of discharges in stellarators to exhibit turbulent fluctuations at magnetic fields which depend on the ion mass, M_i, has been observed.[14] The critical field B_c, for onset of turbulence scales roughly as $M^{1/2}$. In this case we have not determined the critical fields, but we can reliably predict that at higher magnetic fields the Xenon discharge would be turbulent too. (We produced a few discharges in Helium which were also turbulent.) We can also predict that at higher magnetic fields it would be difficult to suppress the fluctuations in WIIa in the contact ionization regimes. Low frequency fluctuations can also be expected for lighter mass alkali and alkaline earth plasmas produced by contact ionization in the present magnetic field range.

The almost monochromatic oscillations in the Xenon discharges are interesting candidates for experiments on feedback stabilization.

7. Scaling with magnetic field

A few data were obtained using microwave oscillators at 13.3 and 15.7 GHz. Figure 15 shows data on density versus magnetic field at the same power level. The trend shows an increase in density with increasing magnetic field which is in the correct direction, but the absolute power measurements must be improved before this type of comparison can be made quantitative. An adequate theory of the energy balance in this type of discharge is also lacking. The power levels in Figure 15 were measured at the oscillators and do not take into account losses in the waveguides or the mismatch at the vacuum window.

8. Trapped particle effects

The electron-neutral and electron-electron mean free paths shown in Table I are comparable with or larger than the circumference of WIIa and the effects of trapped particles on diffusion should be estimated. This is difficult because the theories of trapped particle diffusion in stellarators are crude, at best, and even these apply to unrealistic limiting cases. Thus, the results are probably qualitatively correct but not very accurate. We will base our estimates of the diffusion due to trapped particles on the estimates for axisymmetric systems because the range of collision frequencies in these discharges indicate that the particles are trapped in the toroidal field but not in the helical fields.

We know the so called neo-classical diffusion coefficient D_{nc} to be given by the Galeev-Sagdeev[15] plateau value

$$D_{nc} \approx \frac{57}{t} \cdot \frac{r_{ge}}{R} \cdot D_B = 10^{-2} \cdot D_B$$

if we take $t = 0.2$, $R = 50$ cm, $B = 3.3$ kilogauss, and $T_e = 5$ eV. The Bohm diffusion coefficient D_B, calculated for $T_e = 5$ eV and $B = 3.3$ kilogauss is $D_B = \frac{1}{16} \frac{ckT}{eB} \approx 10^4 \text{cm}^2 \text{ sec}^{-1}$.

If we substitute the parameters given above into the diffusion coefficient derived by Kovrizhnik[16] for weakly ionized plasmas we obtain about the same value as that given by D_{nc}. Hence, the estimates of diffusion coefficients which take into account the effects of particles trapped in the toroidal field (banana orbits) are in agreement for both electron-ion and electron-neutral collision. The values of the diffusion coefficients seem to be too small by about an order of magnitude to account for the data given here. However, the possible errors in estimating the diffusion coefficient from the data are such that a more careful and extensive series of measurements is justified.

We note that the estimates of confinement time based on n_e vs t data are almost independent of t for $t > 0.1$ because the density increases slowly as t increases (we obviously refer only to the maximum in density and

not the minima or "holes") while the estimated confinement times obtained from the neo-classical collisional diffusion coefficient become progressively larger as t increases because of the variation of the neo-classical coefficient with t. As for the cases of higher power the density seems to increase less slowly then linearly with power at fixed pressure. Therefore, the largest confinement times occur at lower power levels. For this reason we have made our estimates only for a low power level, low pressure and one value of rotational transform. A more detailed comparison with theoretical estimates of neo-classical diffusion will be given elsewhere [17].

To conclude this section we call attention to Figure 12 and comment that changing the neutral pressure by a factor 30 had a relatively small effect on the confinement times determined from the decays of afterglows. Since the variation of the diffusion coefficient with collision frequency is rather weak in this regime, perhaps this is to be expected.

9. Comparison with other stellarators

The confinement of plasmas with densities in the range $10^9 - 10^{10}$ cm^{-3}, electron temperatures 3-10 eV, and in confining fields of 1-10 kilogauss has been studied in stellarators at several laboratories. [3-8, 17] Unfortunately, the techniques of producing the plasmas varied in the different experiments which means that the inter-comparison of the data is difficult.

Table II shows a summary of results and characteristics obtained from the references mentioned above and the present measurements. An examination of the data of Table II reveals that, with the possible exception of the Model C stellarator, the experiments show confinement times about an order of magnitude larger than the Bohm time.

Unfortunately, the different modes of plasma production make difficult a satisfactory comparison of the various devices. We can only enumerate the following differences: (1) the plasmas produced in L-1, Etude, and Proto-Cleo were produced by guns of various types which means that the ions were much more energetic than the cold ions produced in weakly

ionized ECR plasmas; (2) the Model C ECR plasmas were produced in a device with a divector which means that the magnetic topography was significantly different; and (3) the Etude and Model-C stellarators are of "race track" form while the others are circular tori.

The low power ECR plasma production in stellarators as described herein would seem to be a suitable technique for comparing devices. For example, measurements can be made of the steady state density as a function of t at various confining fields and neutral pressures for calibrated microwave power levels, as the example in Fig. 3. This procedure would provide a set of standard comparison data.

10. Summary and Conclusions

We have made preliminary measurements of properties of plasmas produced by ECR in the WIIa stellarator. The plasmas were produced in Argon and Xenon, the electron temperatures were in the range 4-11 eV and maximum densities in the range 5×10^8 cm^{-3} to 5×10^{10} cm^{-3}. The general features of the density versus transform curves are quite similar to those observed for Barium plasmas produced by contact ionization. In particular the pattern of minima at the rational values of t was observed which implies that this pattern is a property of the magnetic field rather than the method of production of plasma. The confinement time is estimated to be about 10 Bohm times and certainly less than 100 Bohm times. The confinement does not seem to be explained by trapped particle effects. The discharges in general, are turbulent and show fluctuations in the range expected for drift waves.

For this range of discharge parameters we conclude that confinement in the WIIa stellarator is quite similar to that of Proto Cleo at Culham, Etude and Model C at Princeton, and L-1 at Lebedev. This experiment does not permit us to determine the scaling with magnetic field. The extension of these measurements to other magnetic fields and gases seems desirable.

11. Acknowledgments

We gratefully acknowledge the assistance of Mr. Gronmeyer, who constructed the probes; Mr. Lankes and Mr. Leitl who operated the stellarator; Mr. Zippe who provided assistance with electronic circuits, and Mr. Rossetti and Mr. Capitanio who assisted with the microwave circuits.

One of us (R.A.E.) would like to express his appreciation for the hospitality extended him during his visit to the Institut für Plasmaphysik at Garching while this research was carried out.

References

1 E. Berkl, et al., Phys. Rev. Letters, 17, 906 (1966).

2 E. Berkl et al., in Plasma Physics and Controlled Nuclear Fusion Research (International Atomic Energy Agency, Vienna, 1969), Vol. 1, p. 513.

3 R. Ellis and H. Eubank, Phys. Fluids 11, 1109 (1968).

4 D.K. Akalina, et al., in Plasma Physics and Controlled Nuclear Fusion Research (International Atomic Energy Agency, Vienna, 1966), Vol. 3, p. 733.

5 M. Berezhetosky, et al., in Proceedings Third European Conference on Controlled Fusion and Plasma Physics (Walters-Noordhoff Publishing, Utrecht 1969), p. 5.

6 D.J. Lees et al., in Proceeding Third European Conference on Controlled Fusion and Plasma Physics (Walters-Noordhoff Publishing, Utrecht 1969), p. 4.

7 V. Bocharov et al., in Plasma Physics and Controlled Thermonuclear Research (International Atomic Energy Agency, Vienna, 1969), Vol. 1, p. 561.

8 J. Gorman et al., Phys. Rev. Letters, 22, 16 (1969).

9 J. La Framboise, UTIAS Report No. 100, June, 1966 Univ. of Toronto, Canada.

10 D. Eckhartt et al., in Proceedings Third Conf. on Controlled Fusion and Plasma Physics (Walters-Noordhoff Publishing, Utrecht, 1969) p. 1.

11 For a plot of the constant B lines in a $\ell = 2$ stellarator see D.K. Akalina et al., Soviet Physics JETP, 29, 391 (1969). The constant-B lines in WIIa are, of course, different, but the complexity is similar.

12 W. Lotz, IPP 1/62 May, 1967 (Institut für Plasmaphysik, Garching bei München).

13 T. Stringer, in Plasma Physics and Controlled Nuclear Fusion Research, (International Atomic Energy Agency, Vienna, 1966) Vol. 1, p. 571.

14 R. Ellis, K. Bol, and T. Stix, Phys. Fluids, 10, 2695 (1967).

15 A. Galeev and R.Z. Sagdeev; Soviet Physics, JETP, 26, 233 (1968).

16 L. Kovrizhnik, Soviet Physics JETP, 29, 475 (1969).

17 To be published as IPP-Report.

18 K. Young and W. Stodiek, Private communication.

Table I

Properties of ECR discharges in Argon

		40 mW (9.2 GHz)	400 mW (13.3 GHz)	4 W (13.3 GHz)
	n_e	$= 3.8 \ldots 9 \cdot 10^8$ cm^{-3}	$6.3 \cdot 10^9$ cm^{-3}	$2 \cdot 10^{10}$ cm^{-3}
	T_e	$= 7 \ldots 9$ eV	7.4 eV	11.5 eV
	λ_{eo}	$= 3 \cdot 10^3$ cm	$2.5 \cdot 10^3$ cm	$1.4 \cdot 10^3$ cm
$6\text{-}8 \times 10^{-6}$	λ_{ee}	$= 1 \ldots 4 \cdot 10^5$ cm	$1.7 \cdot 10^4$ cm	$1.3 \cdot 10^4$ cm
	τ_{ee}	$= 0.6 \ldots 2.2$ ms	0.1 ms	0.06 ms
	$\frac{n_e}{n_o}$	$= 2 \ldots 3 \cdot 10^{-3}$	$2.3 \cdot 10^{-2}$	$6.5 \cdot 10^{-2}$
	τ	$= 1 \ldots 2.9$ ms	0.8 ms	
	τ_B	$= 0.18$ ms	0.26 ms	
	n_e	$= 6.9 \cdot 10^8$ cm^{-3}	$2 \cdot 10^9$ cm^{-3}	$1.2 \cdot 10^{10}$ cm^{-3}
	T_e	$= 5.5$ eV	4.4 eV	4 eV
	λ_{eo}	$= 1 \cdot 10^2$ cm	$1.3 \cdot 10^2$ cm	$1.3 \cdot 10^2$ cm
2×10^{-4}	λ_{ee}	$= 10^5$ cm	$2.5 \cdot 10^4$ cm	$2.7 \cdot 10^3$ cm
	τ_{ee}	$= 0.7$ ms	0.2 ms	0.02 ms
	$\frac{n_e}{n_o}$	$= 8 \cdot 10^{-5}$	$3 \cdot 10^{-4}$	$1.6 \cdot 10^{-3}$
	τ	=	0.1 ms	
	τ_B	=	0.44 ms	

Table II

Comparison of Confinement in Stellarators

Device	Mode of Production	ℓ	Minor Radius (cm)	Major Radius (cm)	B (kG)	T_e (ev)	n_e (cm^{-3})	$\left(\frac{\tau}{\tau_B}\right)_{max}$
Etude [3]	gun	3	3.5	30	$\lesssim 8$	~ 5	10^9	~ 20
Proto-Cleo [6]	gun	3	5	40	$\lesssim 3$	~ 5	10^{11}	~ 20
L-1 [5]	gun	2	4	50	2-10	~ 10	10^{11}	~ 10
Novosibirsk [7]	R-F Stochastic	3	5	50	< 3	~ 5	10^{10}	~ 10
WIIa (this report)	ECR	2	5	50	3.3	5-10	10^{10}	~ 10
Model C [18]	ECR	3	5	108	< 35	5	10^{10}	≤ 6

Figures

Fig. 1 Plan view of the WIIa stellarator.

Fig. 2 The microwave circuit used in these experiments is shown with calibration data for some of the components.

Fig. 3 A curve of density (ion saturation current to a Langmuir probe) vs t for Argon.

Fig. 4 The variation of density and temperature with radius for fixed t.

Fig. 5 Plot of width of radial density distributions as a function of t at fixed microwave power.

Fig. 6 Electron density, n_e at magnetic axis vs microwave power in Argon discharges at fixed t.

Fig. 7 Electron temperature, T_e, versus microwave power in Argon discharge at fixed t.

Fig. 8 n_e vs t plot in Xenon which shows maximum near rational values of t.

Fig. 9 Plot of radial variation of T_e, n_e, and production rate, $S = n_e n_o \overline{\sigma v}$ for an Argon discharge.

Fig. 10 Oscillographs of the decay of ion saturation current after switching off the microwave power in Argon for various values of t.

Fig. 11 Plots of containment time τ vs t for Argon discharge. These values were obtained from the afterglows of ECR plasmas. Also shown is a plot of n_e just prior to termination of the discharges vs t.

Fig. 12 τ vs t for several pressures of Argon. These τ values were obtained from decays of afterglows.

Fig. 13 Spectra of density fluctuations in ECR discharges in Argon for various values of t.

Fig. 14 Spectra of density fluctuations in ECR discharges in Xenon for various values of t.

Fig. 15 n_e on axis vs magnetic field for discharges produced at the same power level by ECR at three different magnetic fields.

PLAN VIEW OF STELLARATOR W II a

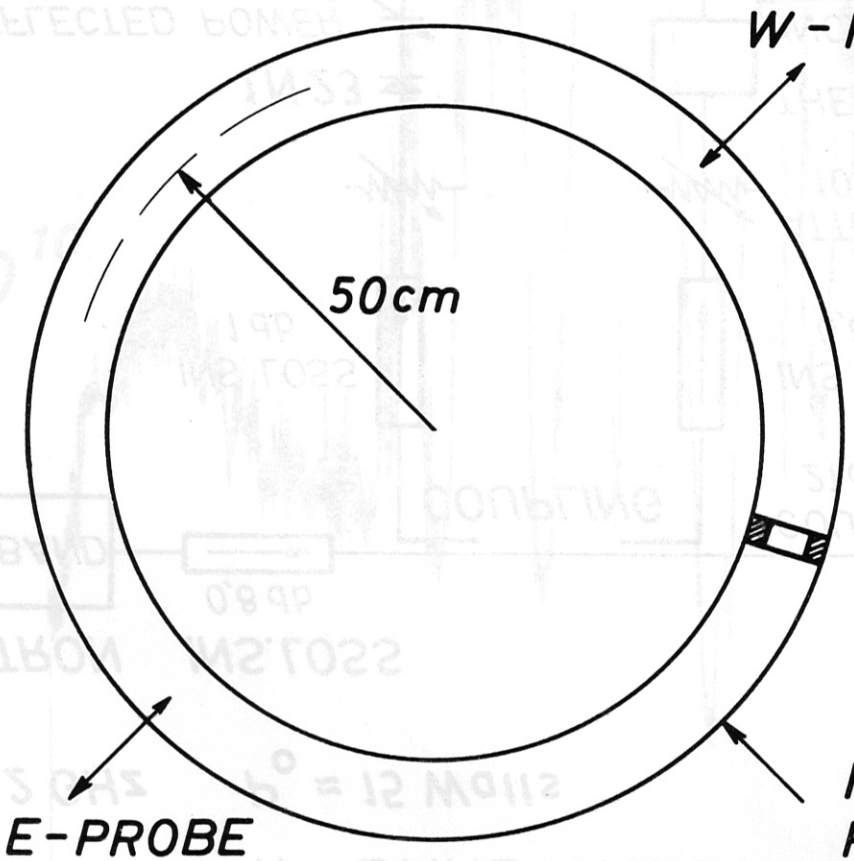

FIG. 1

X - BAND - TRANSMITTER

$f = 9{,}2$ GHz $P_o \approx 15$ Watts

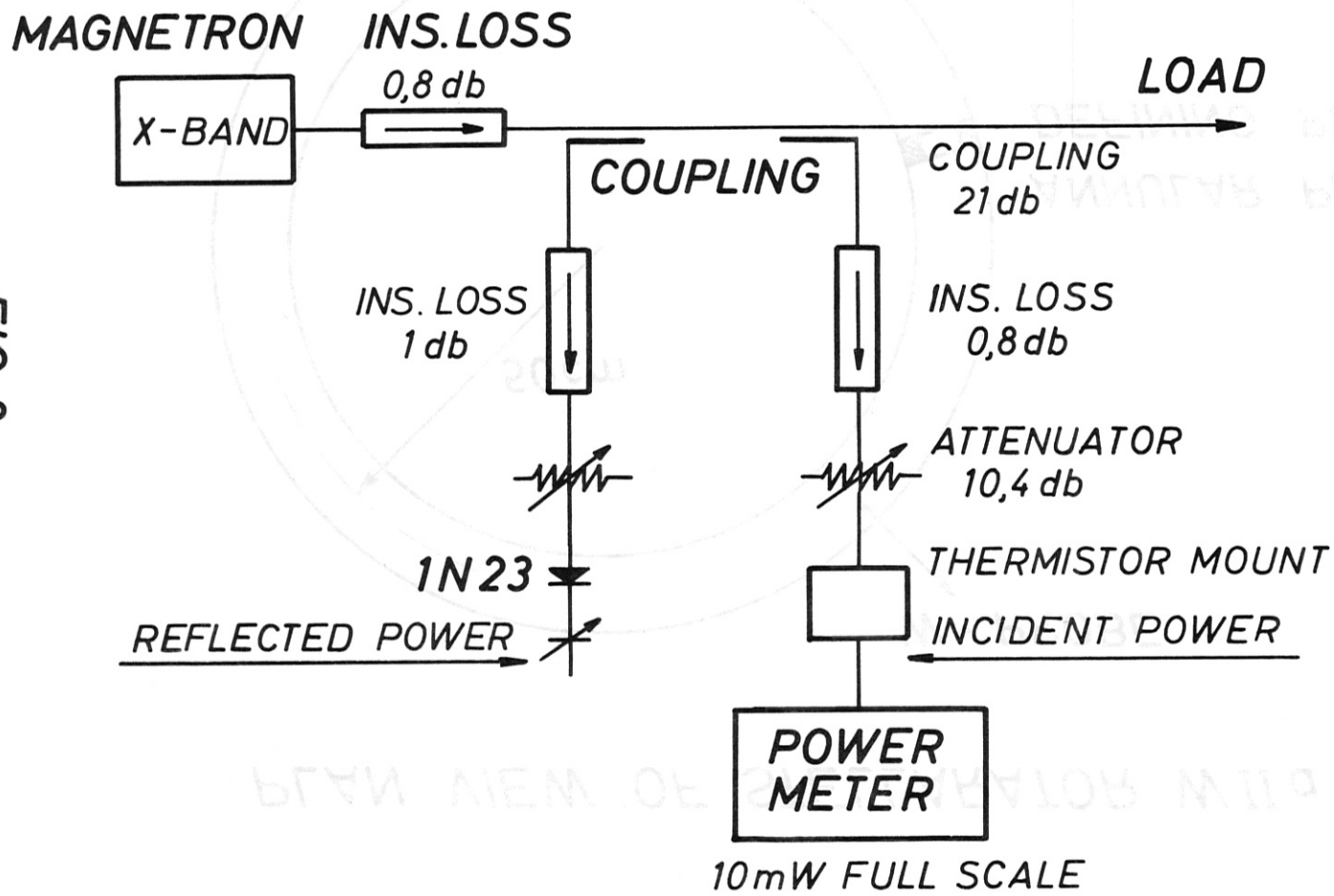

FIG. 2

Power measurement:

0,8	dB	Ins. Loss
21,0	"	Dir. Coupl. Loss
0,8	"	Ins. Loss
22,6	db	
10,4	"	Attennator
33,0	db	

With 33 dB full scale reading: 20 Watts

Maximum uncertainity of data:

by 0,1 mW power range: $\pm 2\%$

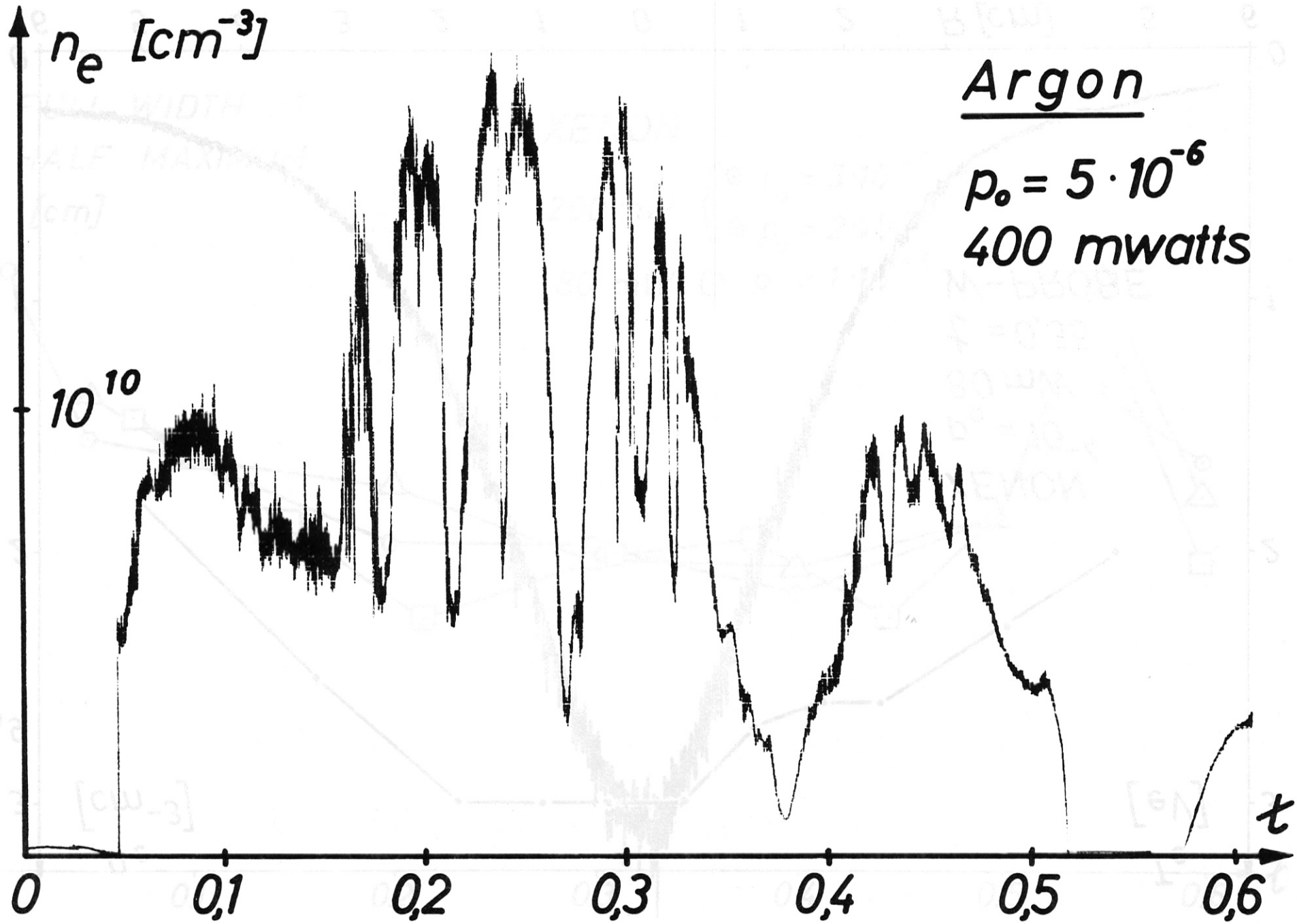

FIG. 3

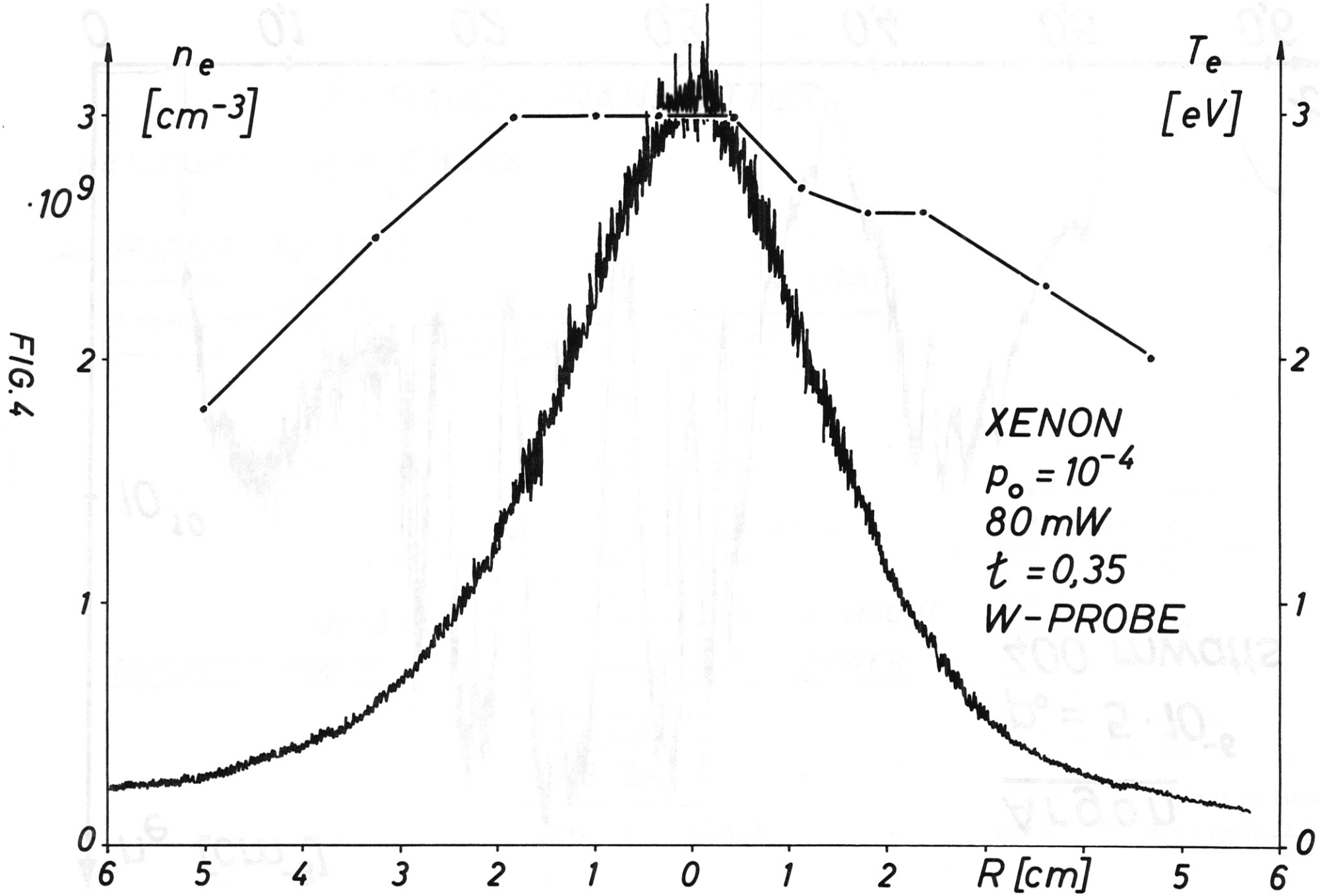
n_e
$[cm^{-3}]$
$\cdot 10^9$
3
2
1
0
T_e
[eV]
3
2
1
0
XENON
$p_o = 10^{-4}$
80 mW
t = 0,35
W-PROBE
6
5
4
3
2
1
0
1
2
R [cm]
5
6

FIG. 4

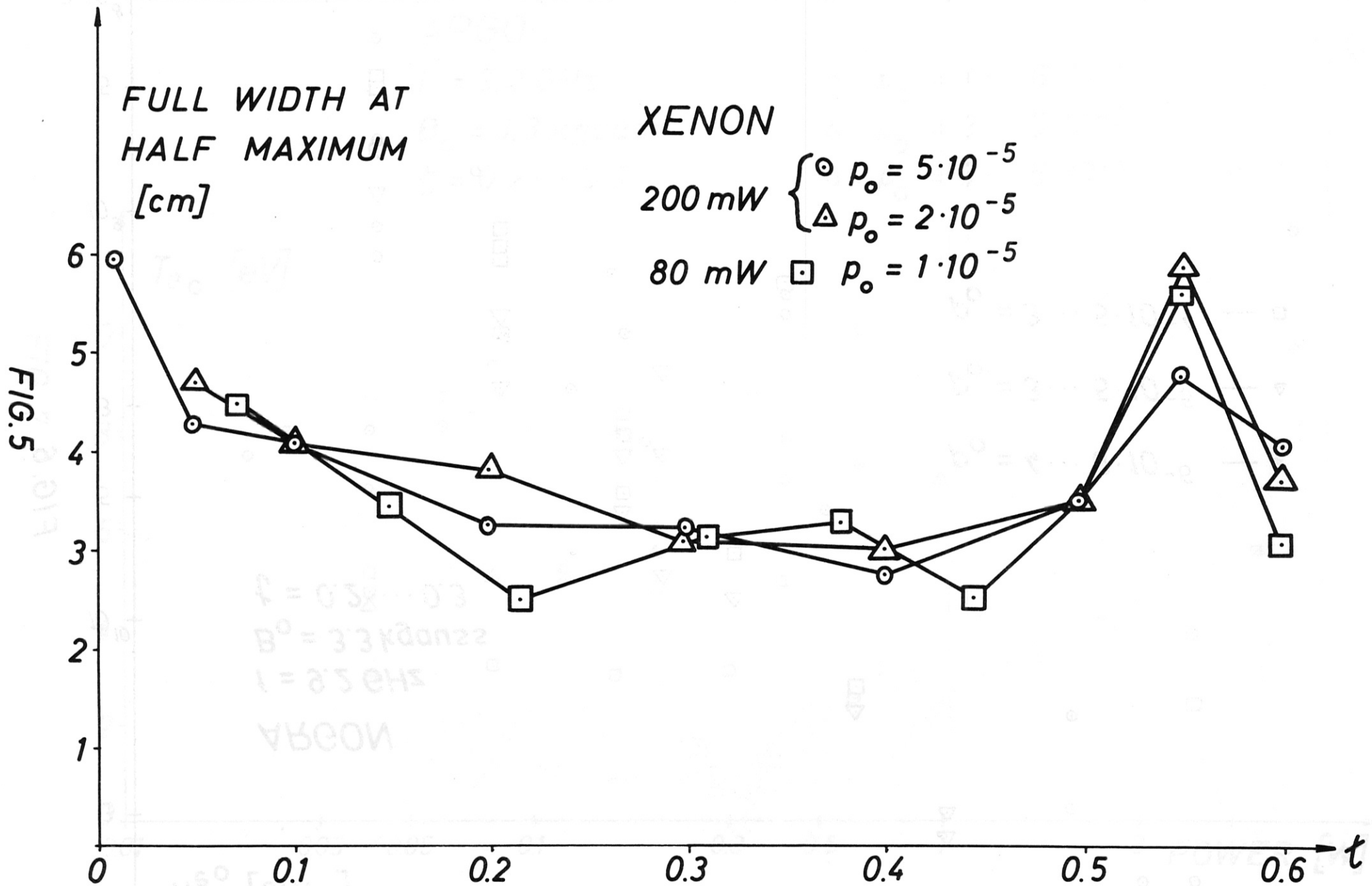
FULL WIDTH AT
HALF MAXIMUM
[cm]
XENON
200 mW
$p_o = 5 \cdot 10^{-5}$
$p_o = 2 \cdot 10^{-5}$
80 mW
$p_o = 1 \cdot 10^{-5}$
6
5
4
3
2
1
0
0.1
0.2
0.3
0.4
0.5
0.6
t

FIG.5

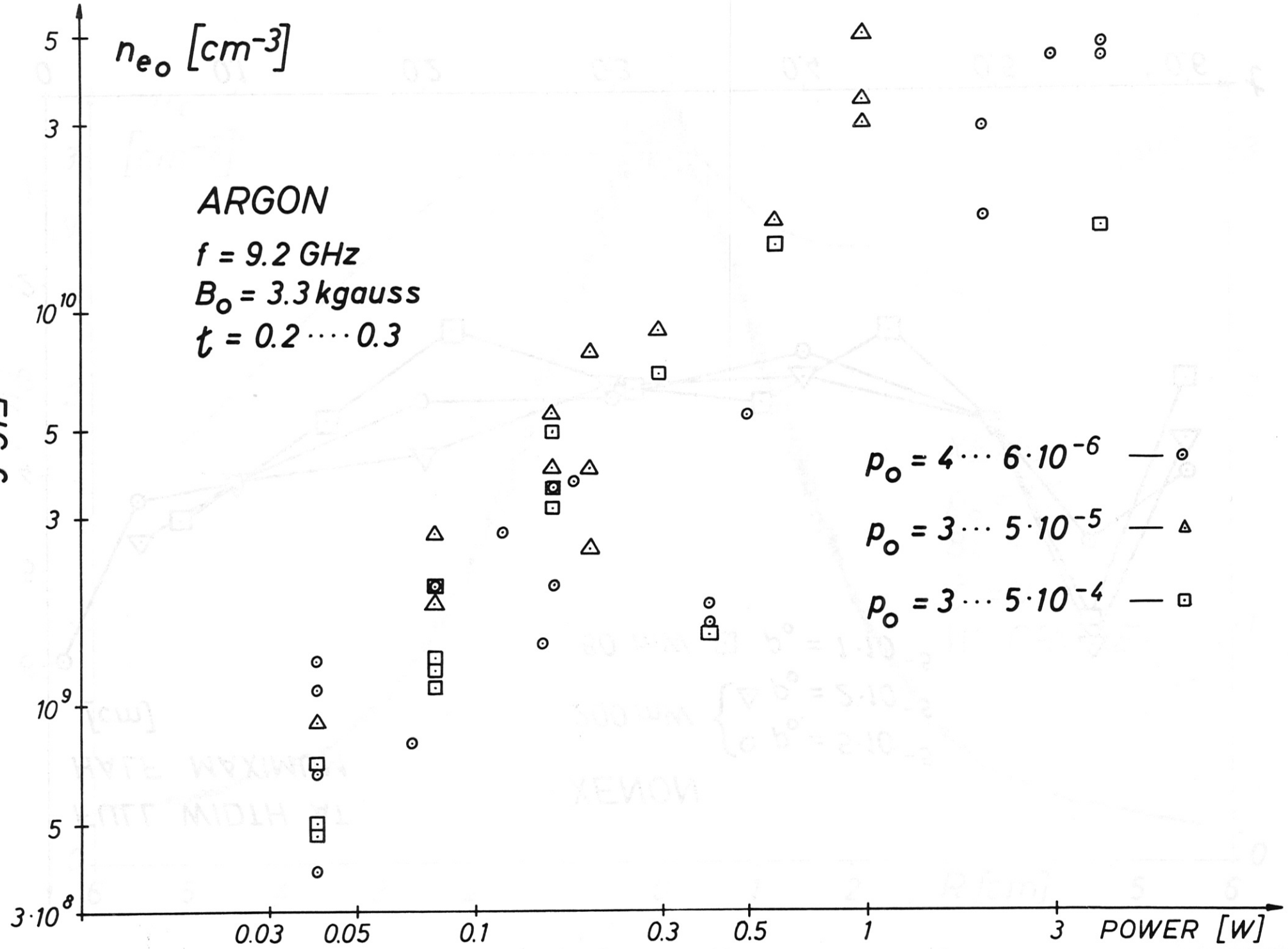
n_{e_o} [cm^{-3}]
5
3
10^{10}
5
3
10^{9}
5
$3\cdot10^{8}$
ARGON
f = 9.2 GHz
B_o = 3.3 kgauss
t = 0.2 ···· 0.3
$p_o = 4 \cdots 6\cdot10^{-6}$ — ⊙
$p_o = 3 \cdots 5\cdot10^{-5}$ — △
$p_o = 3 \cdots 5\cdot10^{-4}$ — □
0.03
0.05
0.1
0.3
0.5
1
3
POWER [W]

FIG. 6

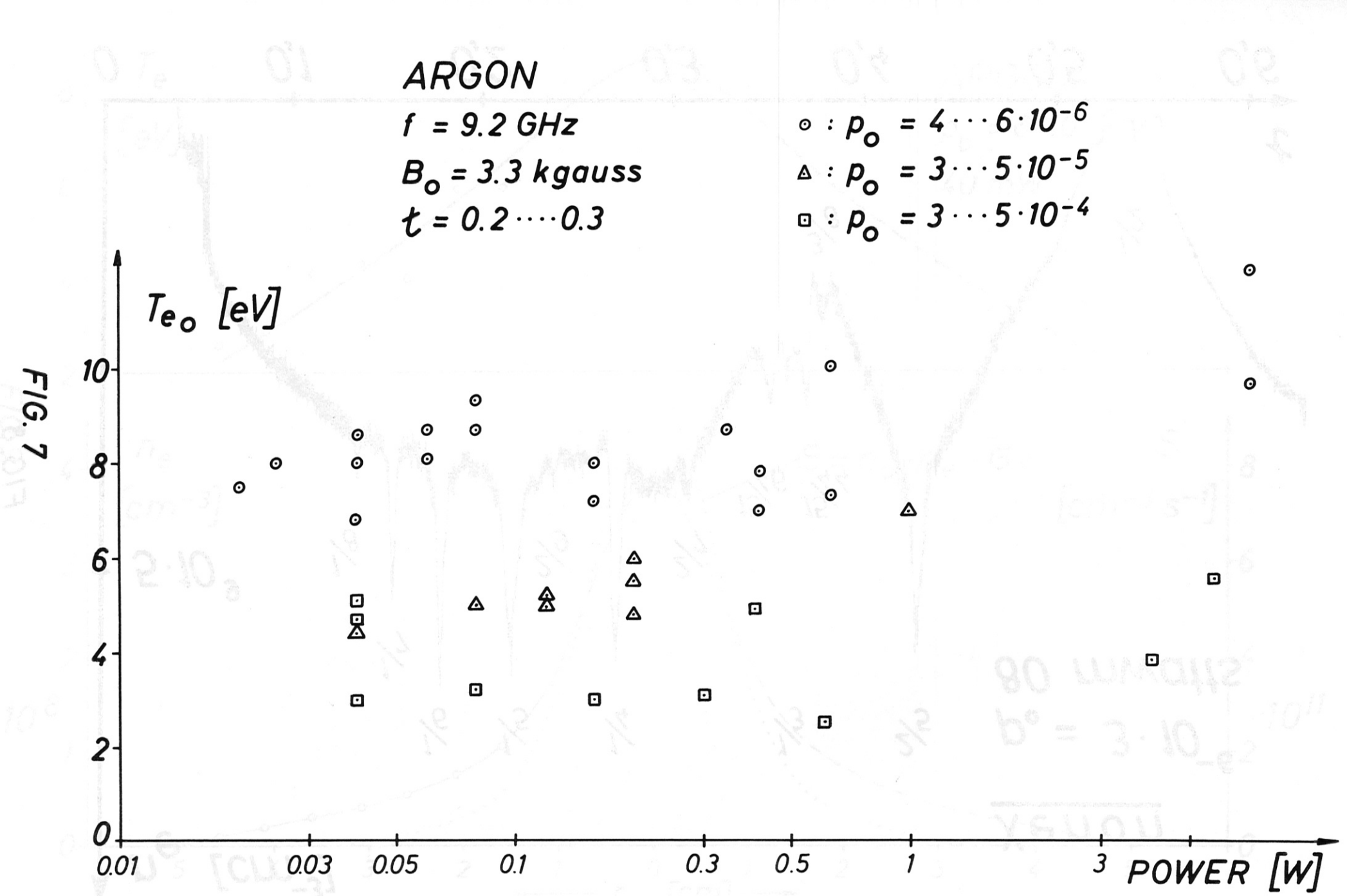
ARGON
f = 9.2 GHz
B_o = 3.3 kgauss
t = 0.2 ···· 0.3
⊙ : p_o = 4 ··· 6·10^-6
△ : p_o = 3 ··· 5·10^-5
⊡ : p_o = 3 ··· 5·10^-4
T_eo [eV]
10
8
6
4
2
0
0.01
0.03
0.05
0.1
0.3
0.5
1
3
POWER [W]

FIG. 7

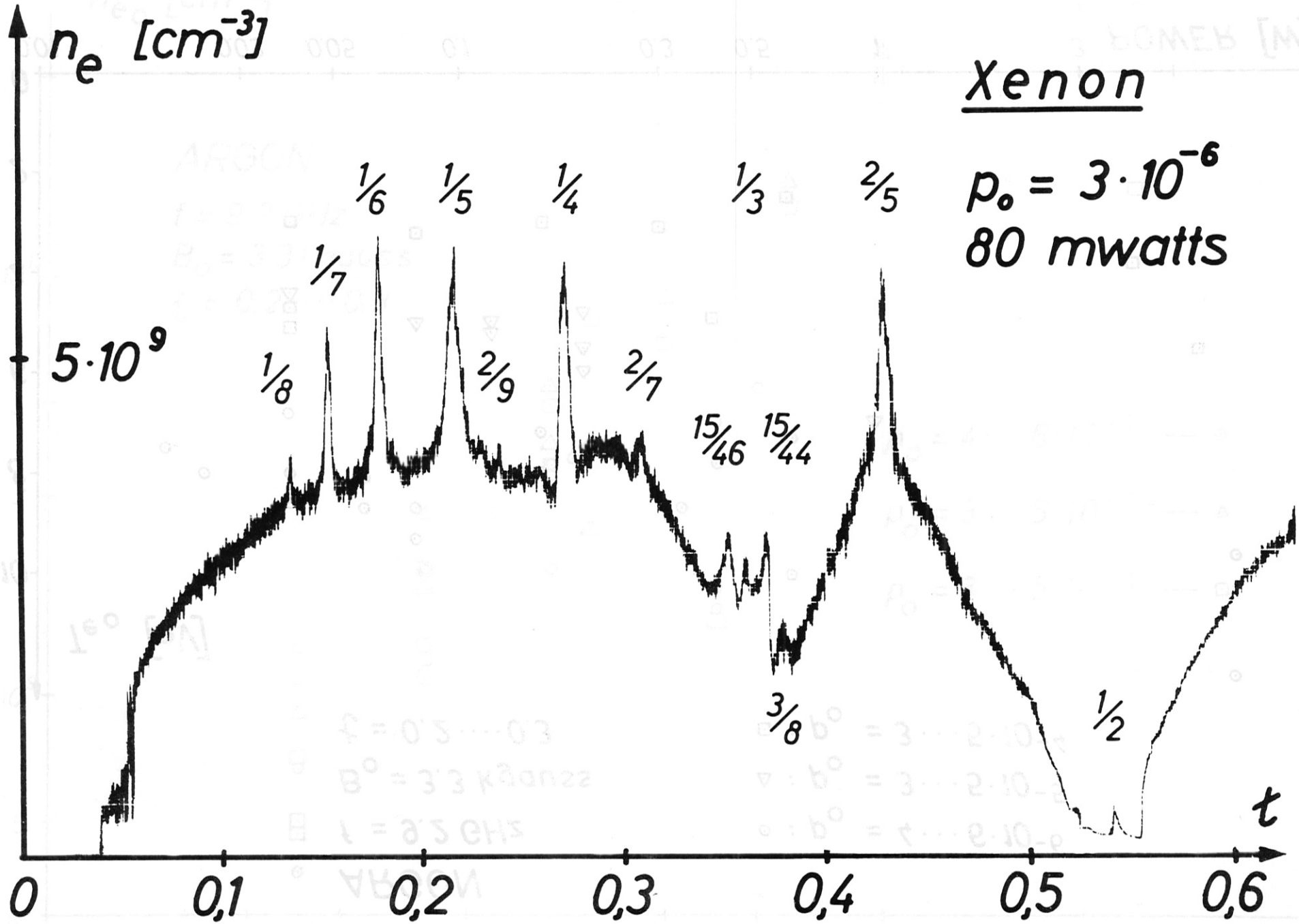
n_e [cm^{-3}]
Xenon
$p_o = 3 \cdot 10^{-6}$
80 mwatts
$5 \cdot 10^9$
1/8
1/7
1/6
1/5
2/9
1/4
2/7
1/3
15/46
15/44
3/8
2/5
1/2
t
0
0,1
0,2
0,3
0,4
0,5
0,6

FIG. 8

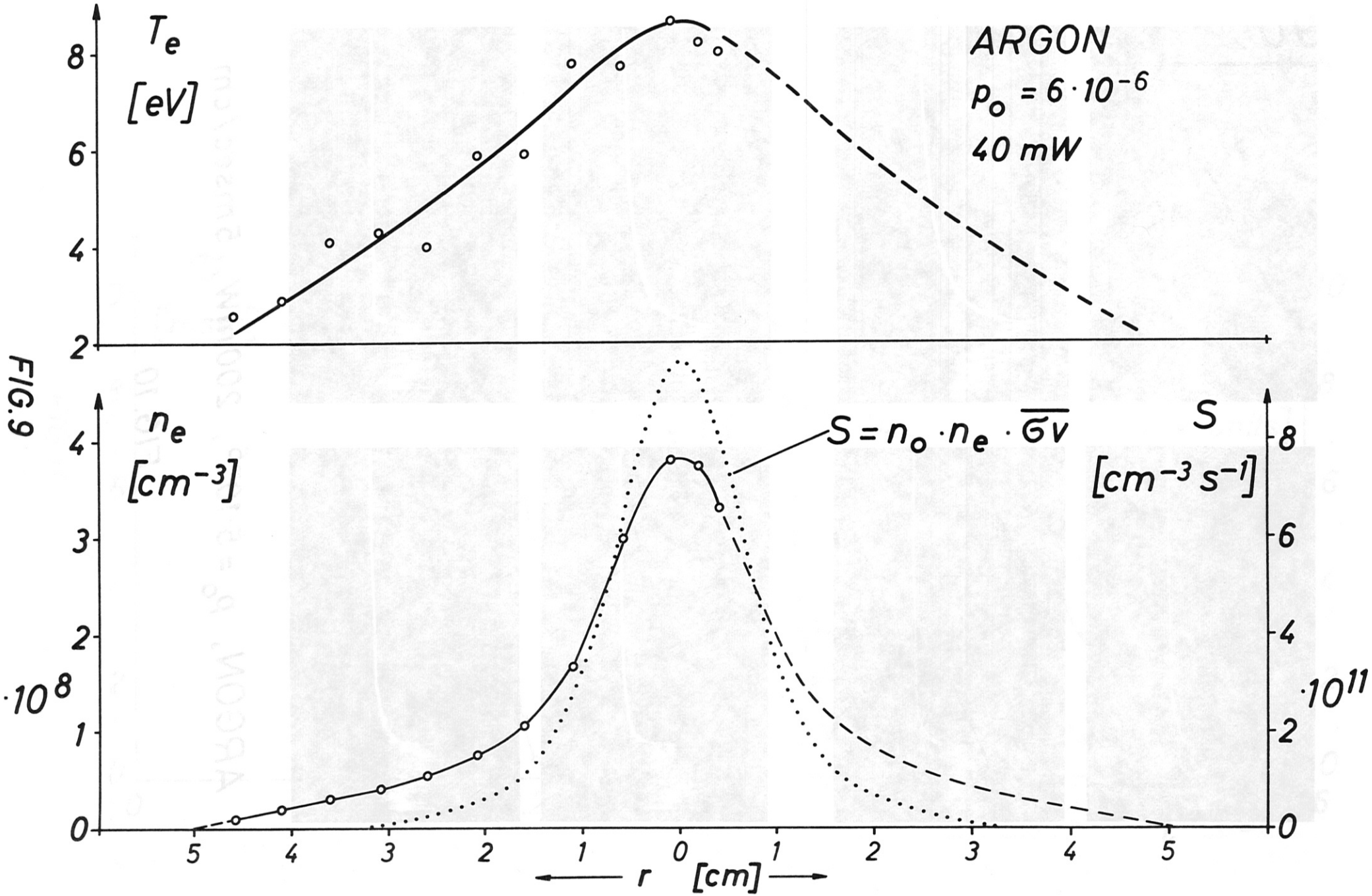
T_e
[eV]
ARGON
$p_o = 6 \cdot 10^{-6}$
40 mW
n_e
[cm^{-3}]
$S = n_o \cdot n_e \cdot \overline{\sigma v}$
S
[cm^{-3} s^{-1}]
$\cdot 10^8$
$\cdot 10^{11}$
r [cm]

FIG.9

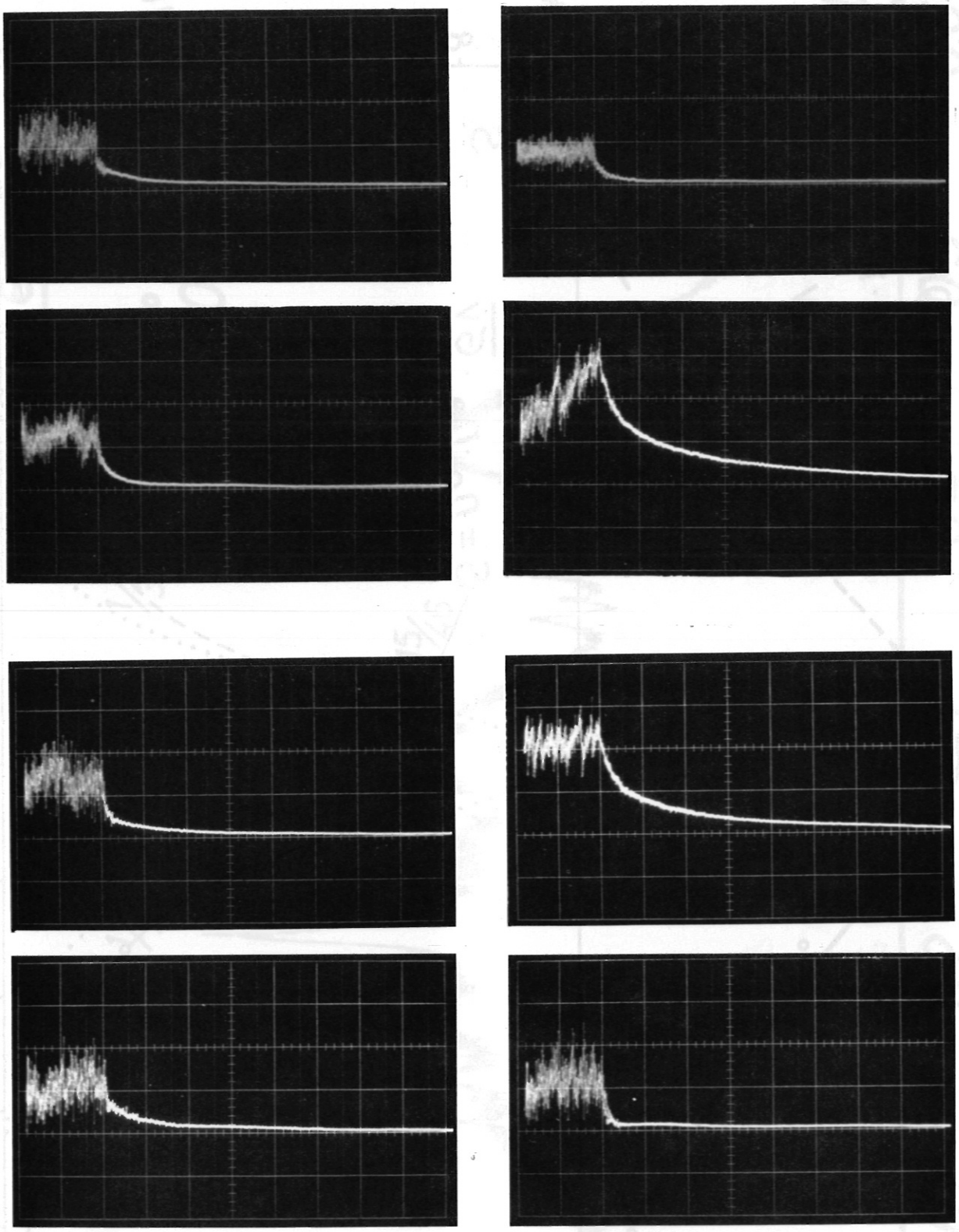

ARGON, $p_o = 5 \cdot 10^{-6}$, 200mW, 5msec/cm

FIG. 10

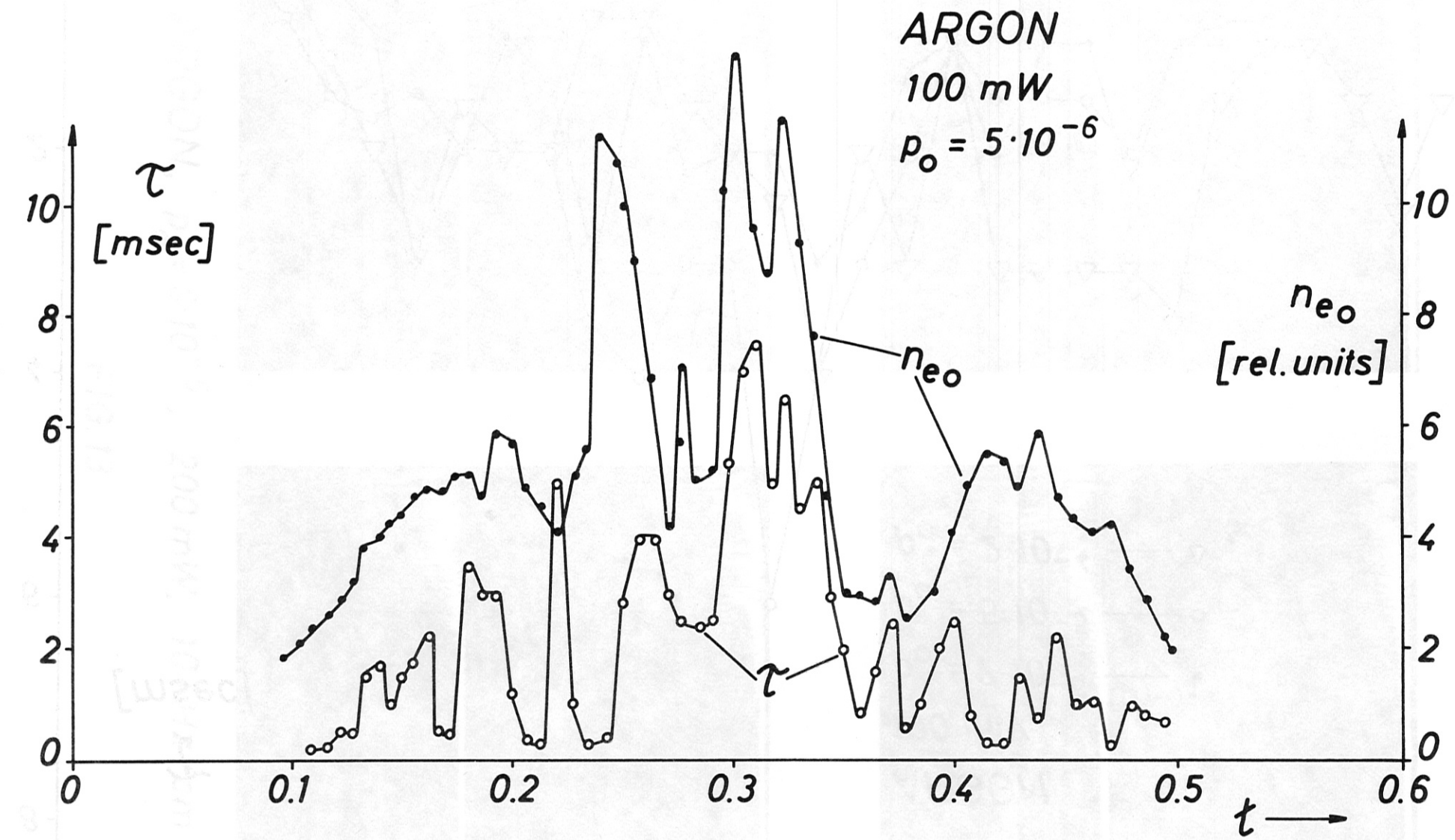
ARGON
100 mW
$p_o = 5 \cdot 10^{-6}$
τ
[msec]
n_{eo}
[rel. units]
n_{eo}
τ
t
0
2
4
6
8
10
0.1
0.2
0.3
0.4
0.5
0.6

FIG. 11

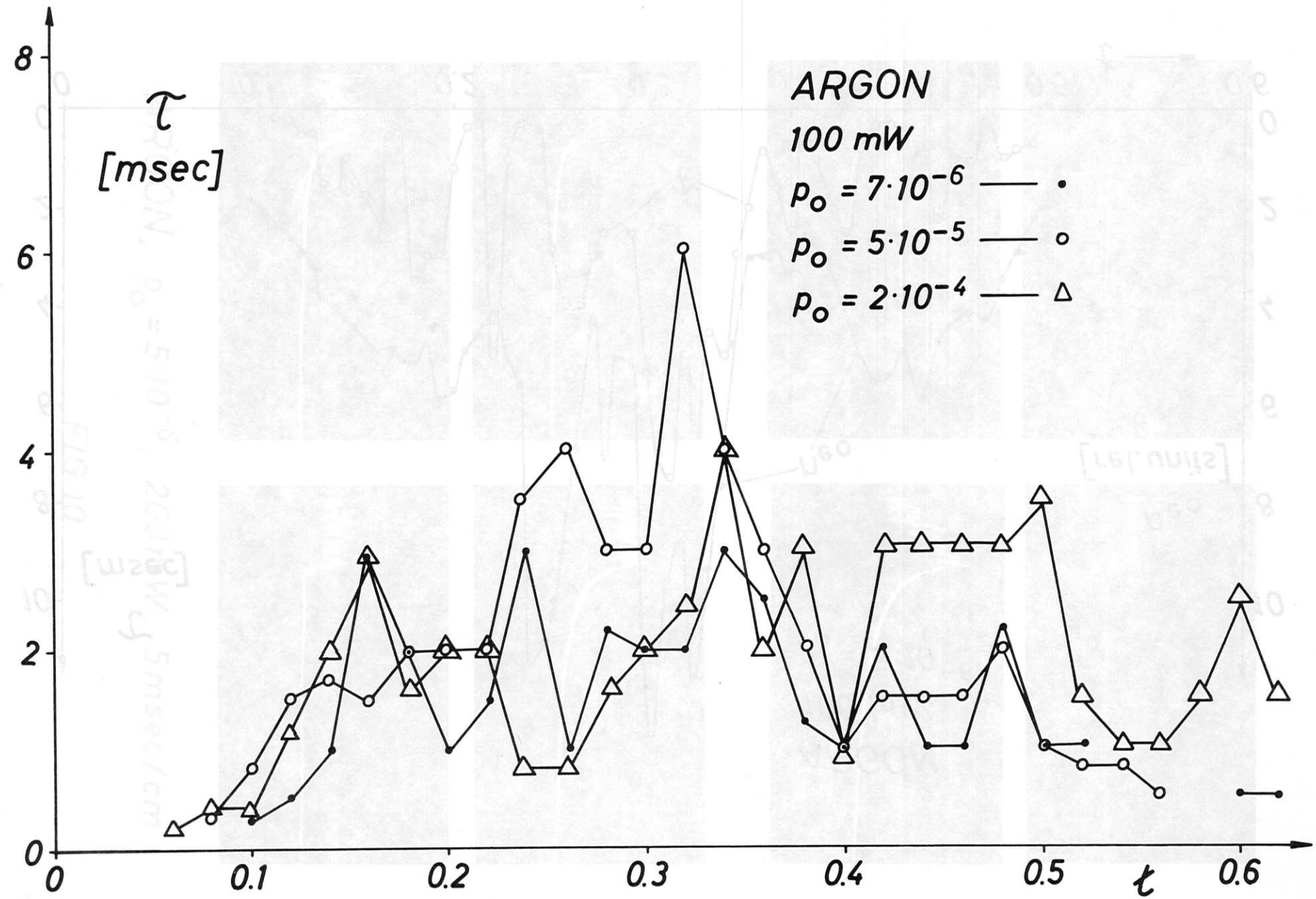
τ
[msec]
ARGON
100 mW
$p_o = 7 \cdot 10^{-6}$
$p_o = 5 \cdot 10^{-5}$
$p_o = 2 \cdot 10^{-4}$
8
6
4
2
0
0
0.1
0.2
0.3
0.4
0.5
0.6
t

FIG. 12

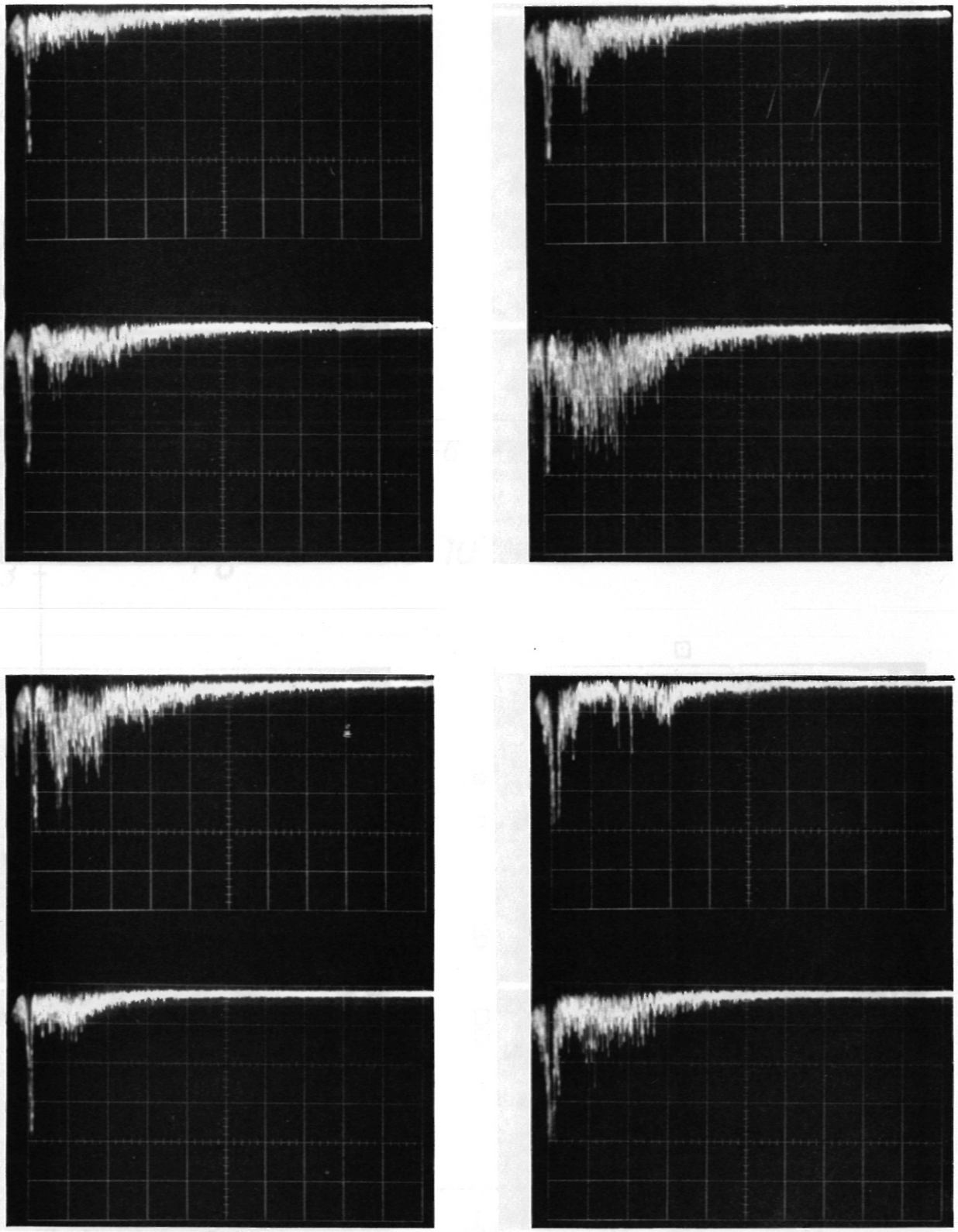

ARGON, $p_o = 6 \cdot 10^{-6}$, 200 mW, 10 kHz/cm

FIG. 13

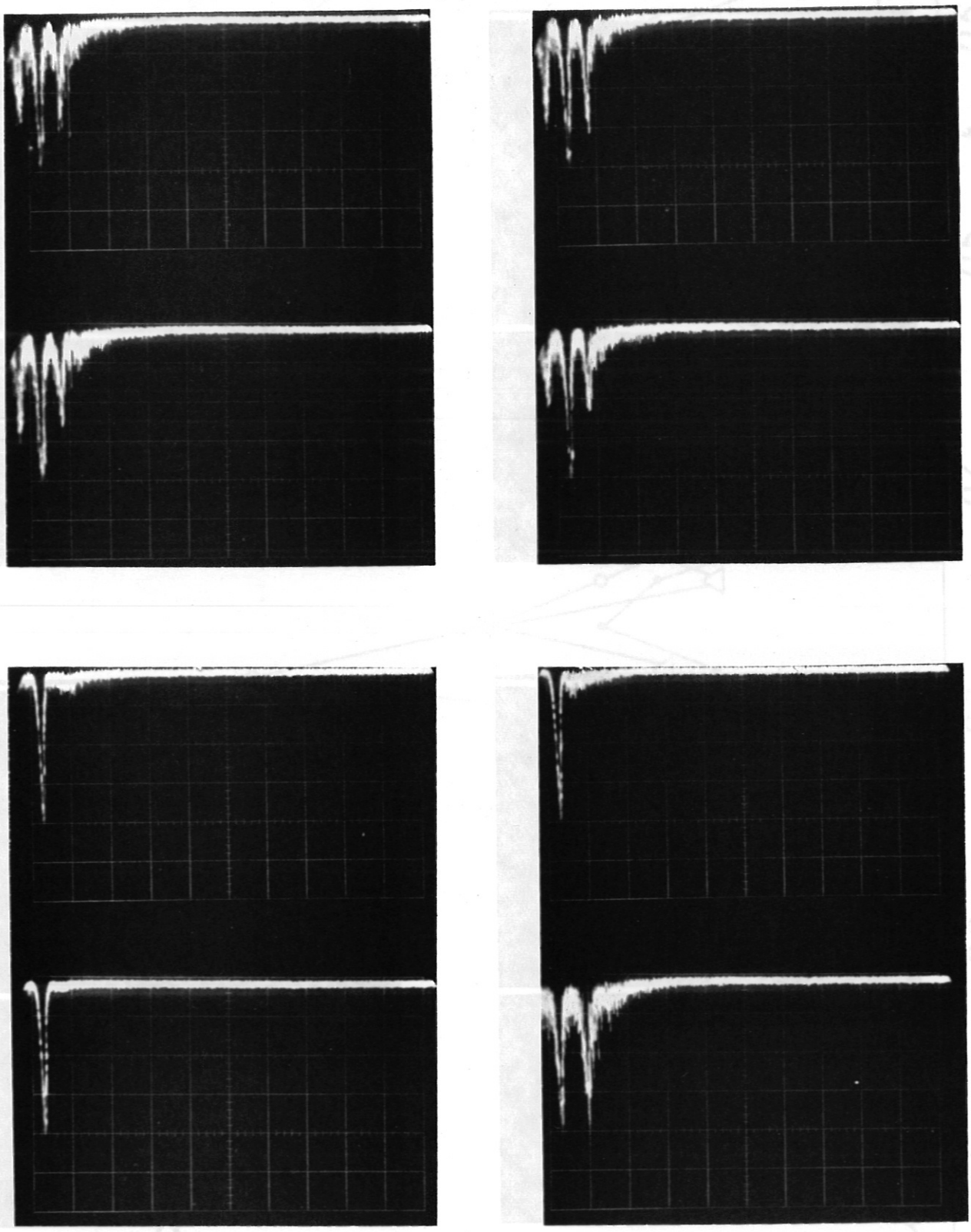

XENON, $p_o = 6 \cdot 10^{-6}$, 60 mW, 10 kHz/cm

FIG. 14

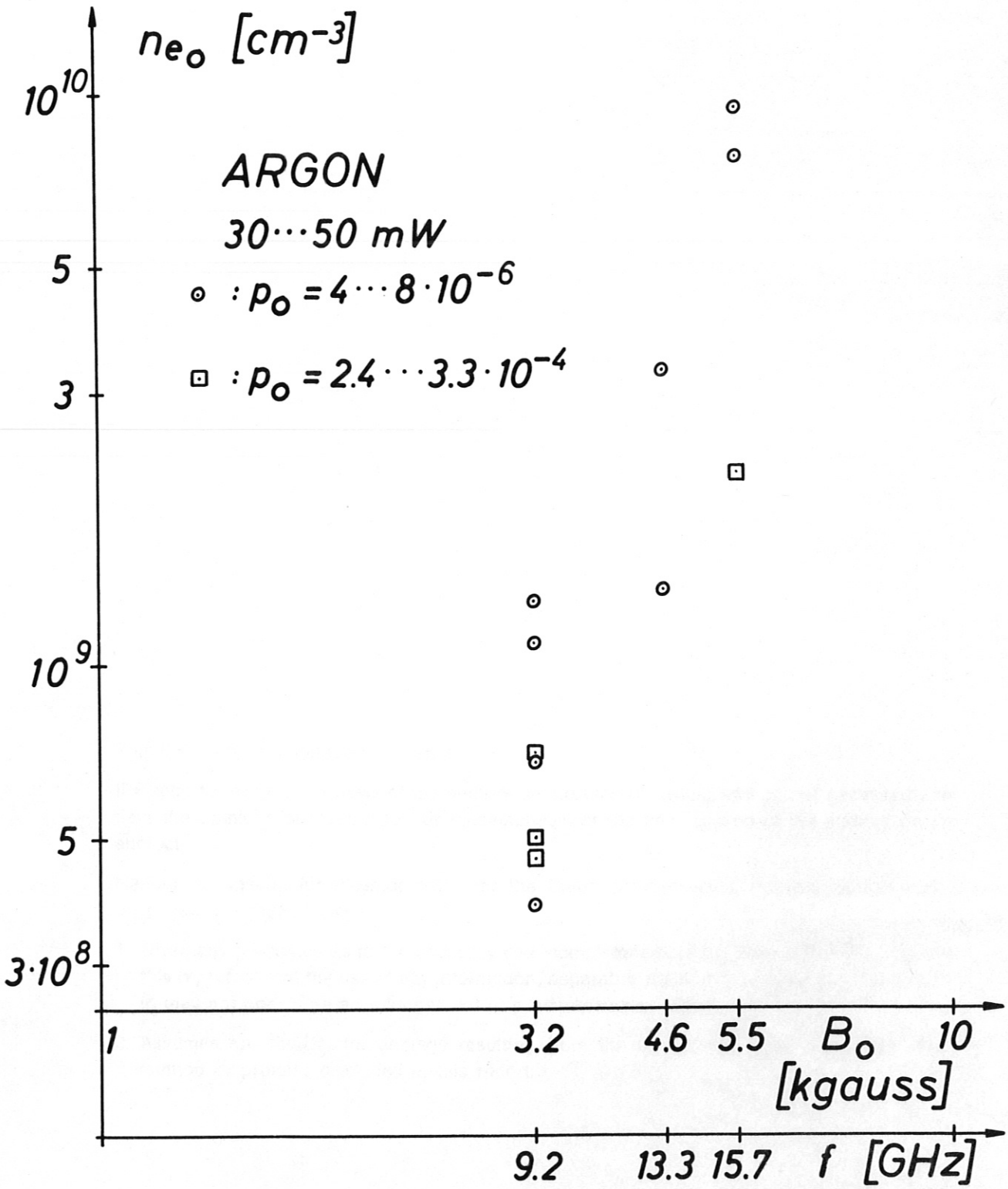
n_{e_o} [cm^{-3}]
10^{10}
ARGON
30···50 mW
5
⊙ : $p_o = 4 \cdots 8 \cdot 10^{-6}$
⊡ : $p_o = 2.4 \cdots 3.3 \cdot 10^{-4}$
3
10^9
5
$3 \cdot 10^8$
1
3.2
4.6
5.5
B_o
10
[kgauss]
9.2
13.3
15.7
f [GHz]

FIG. 15